Proc. of the 8th International Symposium on Geotechnical Safety and Risk (ISGSR)
Edited by Jinsong Huang, D.V. Griffiths, Shui-Hua Jiang, Anna Giacomini and Richard Kelly

doi: 10.3850/978-981-18-5182-7_20-004-cd

ISGSR 2022

A Large Deformation Random Finite-Element Study on the Pull-Out Capacity of Two Typical Offshore Anchors

Shi-Jie Xu[1], Jiang-Tao Yi[2] and Jun Hu[3]

[1]School of Civil Engineering, Chongqing University, P.R. China.
E-mail: Xudetl@cqu.edu.cn
[2]School of Civil Engineering, Chongqing University, P.R. China (Corresponding author).
E-mail: yijt@foxmail.com
[3]College of Civil Engineering and Architecture, Hainan University, P.R. China.
E-mail: hj7140477@hainanu.edu.cn

Abstract: In deep to ultra-deep water developments, various types of offshore anchor provide technically feasible and economically attractive options for mooring systems. Amongst them are the novel self-penetrating torpedo anchor and conventional plate anchor. Subjected to environmental loading, both these types of anchors experience combined vertical (V) and horizontal (H) loading. Moreover, mobilizing their full potentials or maximum pull-out capacities in soft sediments often render soil in the close proximity severely deformed and distorted. It is thus implied that large deformation analyses are warranted to accurately estimate the VH pull-out capacities. Although finite element calculations have been widely reported in the literature to determine the pull-out capacity of torpedo and plate anchors, most of them are small-strain finite element studies. More significantly, the spatial variability or random heterogeneity is rarely taken into account, while there is increasing recognition that the inherent spatial variability of seabed soils can decrease the overall capacity of offshore foundations. This article reports a three-dimensional random finite element study on the pull-out capacities of torpedo and plate anchors, with a view to providing rational interpretation of pull-out mechanism in a spatially variable soil and probabilistic prediction of pull-out capacities. The analysis results show that the soil flow mechanisms over the course of torpedo and plate anchors extraction are apparently affected by the spatial variability of soil. The pull-out capacities in both vertical and horizontal directions are distributed in fairly wide range. Findings in this research may be helpful mainly in that it shed light on the significance of spatial variability on the offshore anchors.

Keywords: anchor; combined loading; spatial variability; Coupled Eulerian-Lagrangian method.

1 Introduction

Torpedo anchor and plate anchor are two typical options for mooring systems in deep and ultra-deep water developments owing to their economic feasibility. A typical torpedo anchor is often rocket shape with a padeye on the top of its shaft, which filled with lead and concrete. And the typical plate anchor consists a fluke, keying flap, a shank fixed with the padeye.

The pull-out capacity of both anchors is the main interest of the mooring system design. During their services, anchors may experience combined uplift vertical loadings from the mooring system, and even the horizontal loadings from the wind, which addresses the importance of understanding the pull-out capacity of anchors in varied direction. For torpedo anchors, O'beirne et al. (2015) proposed a design framework base a series of reduced-scaled field tests and finite element analyses. Hossain et al. (2014), Hossain et al. (2015) also reported the centrifuge test on different pull-out angles for torpedo anchor in kaolin clay and calcareous silts. Finite element studies on the pull-out capacity of torpedo anchor were also reported by Chen et al. (2016), Fu et al. (2017), Fu et al. (2019) and Yi et al. (2020). For plate anchors, extensive studies have been made by model tests and finite element analyses (Chen et al. 2013, Chen et al. 2015, Tho et al. 2014). In these studies the severe disturbances and large deformation of the soil in the vicinity of anchors were widely noticed, which further addressed the necessity of large deformation finite element (LDFE) analysis in pull-out capacity analyses of these two types of anchors.

In field practices, varied types of the anchors are installed in clay which exhibit a strong spatial variety. The influence of spatial variety of soil strength on capacity of various foundations was studied within the framework of finite element analyses in previous studies (Cassidy et al., 2013, Griffiths et al., 2002), and this influence was found significant. Besides, when different direction of the loads were applied, the degree of the influence of spatial variety is different. Cassidy et al. (2013) reported that the variation of horizontal and moment capacity is more significant than which of vertical capacity for strip footing. Li et al. (2017) found that the variation of horizontal capacity is larger than which of vertical capacity for spudcan, owing to that larger volumes of the soil was mobilized when vertical loading was applied. However, most of these random finite element studies were restricted in small strain finite element studying therefore the complicated soil disturbances were missing.

This article presents a three-dimensional large deformation random finite element study on pull-out capacity of two types of anchor. The coupled Eulerian-Lagrangian (CEL) method was adopted to perform LDFE analyses. A humble contribution may be made on the understanding of the effect of spatial variability on the offshore anchors.

2 Methodology

The three dimensional LDFE analyses were conducted by using the commercial software ABAQUS 6.14 (Abaqus, 2014). The torpedo anchor was finless and idealized as a rigid body as its deformation is neglectable. The length of the torpedo anchor is 12 m, with the diameter of 0.762 m, and was wished-in-placed without tilt at the embedment depth (i.e., the distance between the tip of the torpedo anchor and mudline) of 20 m. The dimensions of model is consistent with the field test conducted by O'beirne et al. (2015), detailed dimensions are here given in Figure 1(a). The loading reference point was set on the top of the anchor shaft where the padeye is usually fabricated, and a fixed direction displacement was applied at the loading reference point at a pulling velocity of 0.1 m/s to capture the combined loading failure envelope. The interface friction factor was set equal to the soil sensitivity St, which is equal to 1/3.The soil domain was of 21D in width and 65D in depth (i.e., 16×50 m), which is large enough to eliminate the boundary effect. In the vicinity of the torpedo anchor meshes were refined with uniform sizes (0.1D), while coarser meshes with continuously increasing sizes in further areas were assigned to reduce the amount of elements. According to the mesh convergence study reported by Chen et al. (2013), this mesh density was competent to balance the computational cost and accuracy.

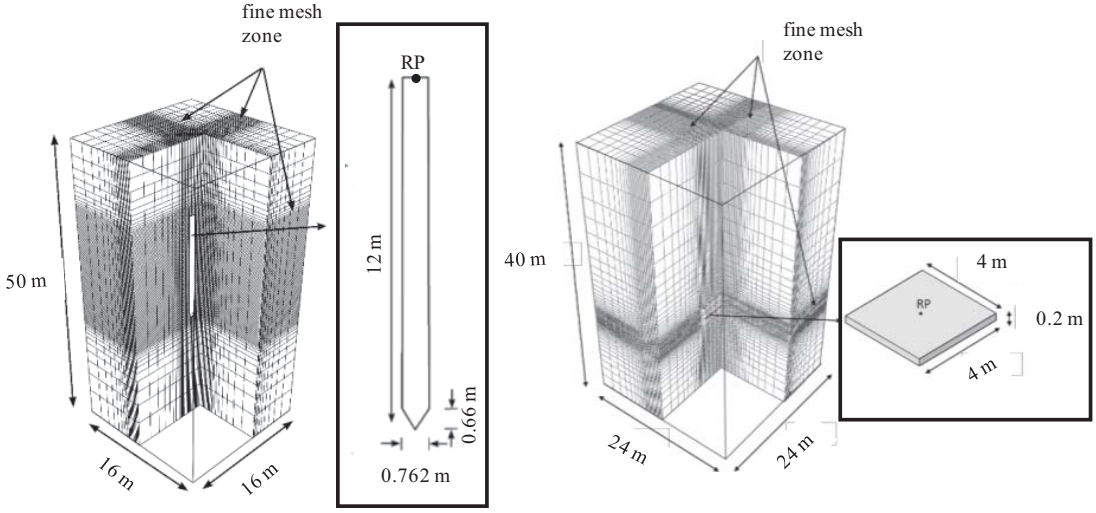

Figure 1. Schematic of finite element models: (a) torpedo anchor; and (b) plate anchor.

In the case of plate anchor, a square shape with 4 m in width B and 0.2 m in thickness, which is consistent with Chen et al. (2013) was chosen in this study and was also modeled as a rigid body. The loading reference point was assigned at the center of the upper surface of the anchor as shown in Figure 1(b). An upward displacement was applied at the loading reference point to model the pull out process of the anchor, and the pull out velocity was set as 0.04 m/s. The square plate anchor was wished-in-place at the embedment depth of 7B (i.e., the distance between the lower surface and the mudline, which is 28 m). The interaction between plate anchor and soil was assumed to be frictionless suggested by Chen et al. (2013). The soil domain was 6B in width and 10B in depth. Note that in both cases, for soil at the boundary, the normal movement to the boundary was restricted and only tangential movement to which was allowed. A fine mesh was also assigned for the region near the anchor, the density of the mesh is consistent with Chen et al. (2013), which is enough for the accuracy requirement. In both torpedo anchor and plate anchor cases, an extended Tresca constitutive model was adopted to account for the strain softening behavior, the undrained shear strength in each point within the model will be upgraded progressively according to its corresponded plastic strain, as shown below:

$$s_{u,mb} = s_{ui}[\delta_{rem} + (1-\delta_{rem})e^{-3\xi/\xi_{95}}] \tag{1}$$

where $s_{u,mb}$ and s_{ui} is the mobilized and intact undrained shear strength, respectively; δ_{rem} is the fully remolded strength ratio (i.e., the inverse of soil sensitivity S_t); ξ is the cumulative plastic strain, ξ_{95} is the cumulative plastic strain required for 95% remolding. In both cases δ_{rem} and ξ_{95} were adopted as 1/3 and 20, respectively. The Young's modulus of soil was set as $500s_{ui}$, and the Poisson's ratio was set as 0.49. For deterministic soil, the linear increasing trend of the soil was accounted, for the intact undrained shear strength s_{ui} at the depth of z, for torpedo anchor case $s_{ui} = 1.5z$ and for plate anchor case $s_{ui} = 5+2z$.

The focus of this study is the effect of the spatial variety of soil undrained shear strength on the pull-out capacity of anchor, the spatial variety of the soil was considered by random fields. The random fields were described by mean value ($\mu_{s_{ui}}$), coefficient of variation (COV) and scale of fluctuation (SOF). The mean value of s_{ui} in random realizations are consistent with the s_{ui} at the same depth in deterministic analysis, namely $\mu_{s_{ui}}=1.5z$ for torpedo case and $\mu_{s_{ui}}=5+2z$ for plate anchor case. Note that the random fields in this study are non-stationary, therefore a conversion from stationary random field to non-stationary random fields are required. Readers may refer Zhu et al. (2017) for the detailed process of this conversion. The modified linear estimation method was utilized to generate a lognormally distribute s_{ui}, readers may refer Liu et al. (2014) for further information on the detailed generation procedure of random field. The COV of s_{ui} in this study was set to be 0.1, 0.3, 0.5; and the SOF was set to be 50.7 m in horizontal direction and 3.8 m in vertical direction. These parameters are within the range reported by Phoon and Kulhawy (1999). As shown in Figure 2(a, b), three random fields with different of COVs are illustrated as a demonstration. Owing to that the vertical SOF is much smaller than horizontal SOF, the s_{ui} of soil fluctuate more rapidly in vertical direction than which in horizontal direction, and a distinct layering pattern can be observed. In each case 400 Monte Carlo realizations were repeated to generate reproducible results.

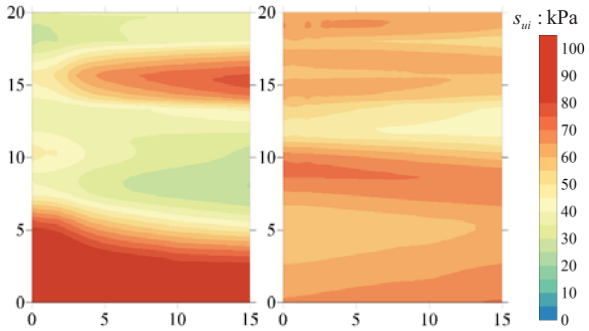

Figure 2. A realization of random field of s_{ui} (a) COV = 0.3, (b) COV = 0.5 (axes in m).

3 Results of Numerical Study

3.1 Deterministic results

In regard to torpedo anchor case, the ultimate pull-out capacity here was defined as the pull-out force when the displacement of padeye u is equal to 0.1 times D of the torpedo anchor, as suggested by API (2011). For simplicity, the horizontal pull-out capacity here will be further discussed to demonstrate the failure mechanism. The load displacement curve is demonstrated in Figure 3(a), where the padeye displacement u was normalized by the diameter of torpedo anchor. The pull-out capacity can be then determined, which is 1000.5 kN, consistent with the calculation suggested by Broms' method (977 kN) in API (2011). The corresponded failure mechanism can be seen in Figure 3(b), a vortex-shaped soil flow around the rotational center can be observed and this observation is consistent with Fu et al. (2019). Figure 4 further illustrated the normalized combined loading failure envelope of torpedo anchor, where the horizontal component of pull-out capacity H was normalized ultimate horizontal pull-out capacity H_0, and vertical component V was normalized by the ultimate vertical pull-out capacity V_0. The results from this deterministic study was comparable with centrifuge results reported by Fu et al. (2017) and numerical result of de Sousa et al. (2011).

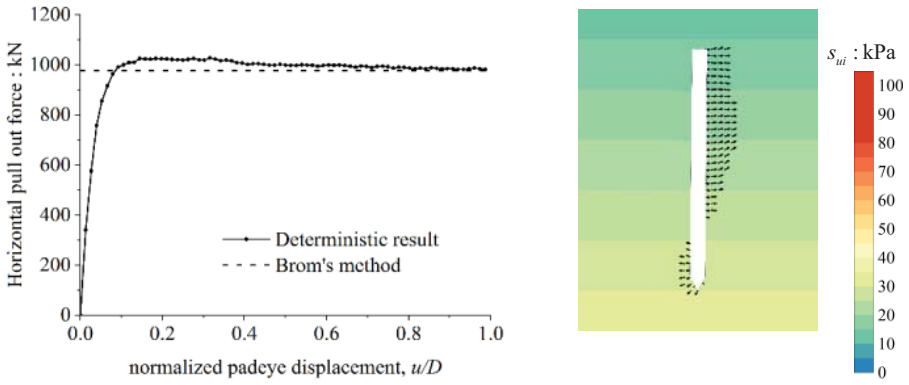

Figure 3. (a) Pull-out capacity vs normalized displacement curves and (b) failure mechanism of the torpedo anchor

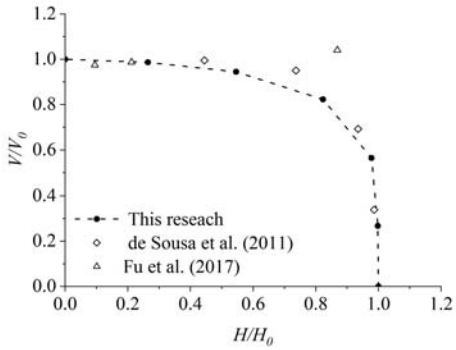

Figure 4. Normalized vertical component vs Normalized horizontal component for torpedo anchor.

In regard to plate anchor, the capacity factor N_c can be calculated by the equation below:

$$N_c = F / As_{ui} \tag{2}$$

Where the s_{ui} is the intact undrained shear strength at the load reference point. The relation between the capacity factor and normalized padeye displacement w/B is illustrated in figure 5(a). It can be seen that the capacity factor converges at around 8.2 when normalized padeye displacement larger than 0.2. In this study the ultimate capacity of the plate anchor was chosen as the capacity when the padeye displacement is equal to 0.5B to guarantee the soil is sufficiently mobilized (the initial embedment depth is 7B). As such the ultimate capacity factor in deterministic study is 8.18, which is consistent with Tho et al. (2014), and the failure mechanism is illustrated in figure 5(b) accordingly, where a cavity (the white color region below the plate anchor) behind the plate anchor can be observed.

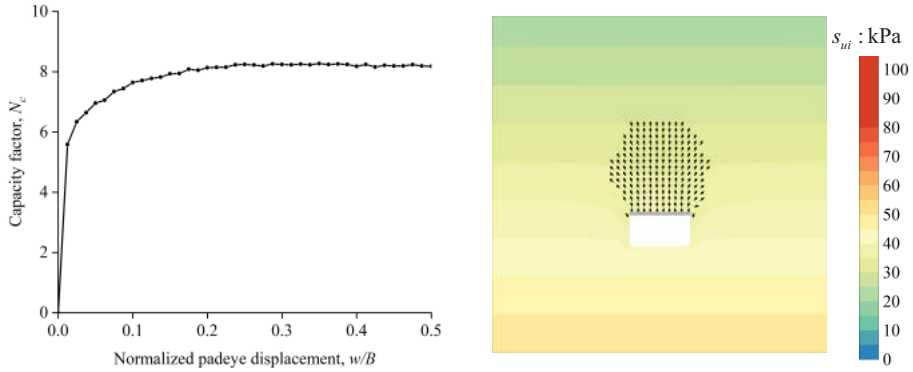

Figure 5. (a) Capacity factor vs normalized displacement curves and (b) failure mechanism of the plate anchor.

3.2 Stochastic Analysis

The typical realization (the COV of s_{ui} is 0.5) is demonstrated respectively, for torpedo anchor and plate anchor a Figure 6(a and b). Visibly in both realizations the soil flow mechanism is largely altered due to the heterogeneity of the soil, which further lead to the variation of the pull-out capability.

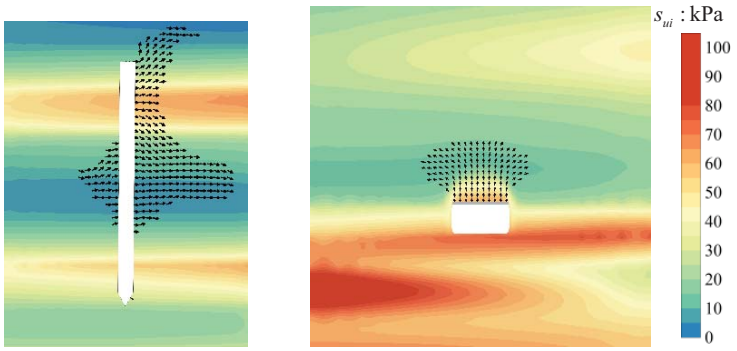

Figure 6. Typical soil flow mechanism in random realization from (a) torpedo anchor (b) plate anchor, where in both realizations COV (s_{ui}) is 0.5

.

For torpedo anchor, in order to derive the probabilistic combined loading failure envelopes, 7 paths of the displacements were applied on the padeye of the anchor in one single realization, a similar procure to Cassidy et al. (2013) was then performed. Firstly, the pull-out capacity in each loading path were initially ranked from the

lowest to the highest by the factor r which determined by the equation below:

$$r = \sqrt{\left(\frac{V_{ran}}{V_{0,det}}\right)^2 + \left(\frac{H_{ran}}{H_{0,det}}\right)^2} \tag{3}$$

Where V_{ran} and H_{ran} are vertical and horizontal component of pull-out capacity, $V_{0,det}$ and $H_{0,det}$ are the vertical and horizontal ultimate pull-out capacity in deterministic analyses. Then the points of 5th percentile in each cluster of points were picked out and connected, as shown in Figure 7. This probabilistic combined failure envelope implies that only 5% of pull-out capacity in the stochastic realizations will locate within this envelope. Furthermore, it can be seen that the envelope shrinkages with the increasing of COV (s_{ui}). With the increasing of COV (s_{ui}), the reduction of $H_{ran}/H_{0,det}$ is more significant than which of $V_{ran}/V_{0,det}$.

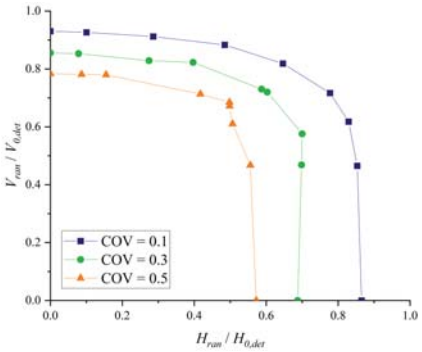

Figure 7. Probabilistic combined loading failure envelope of 5th percentile with deferent of COV (s_{ui}).

For plate anchor, the histogram of capacity factor $N_{c,ran}$ in random realization for various of COV (s_{ui}) is illustrated in Figure 8, and the fitted lognormal distribution curves were also overlaid. Kolmogorov-Smirnov goodness-of-fit tests were conducted and confirmed that the $N_{c,ran}$ with different of COV (s_{ui}) all follow the lognormal distribution. The average capacity factors are 8.13, 7.75, 7.17 for COV (s_{ui}) are equal to 0.1, 0.3 and 0.5 respectively. And the COV of capacity factors are 0.053, 0.16 and 0.27, respectively. With the increasing of COV (s_{ui}), the average of $N_{c,ran}$ in random realizations will decrease and the variance of $N_{c,ran}$ will be more significant.

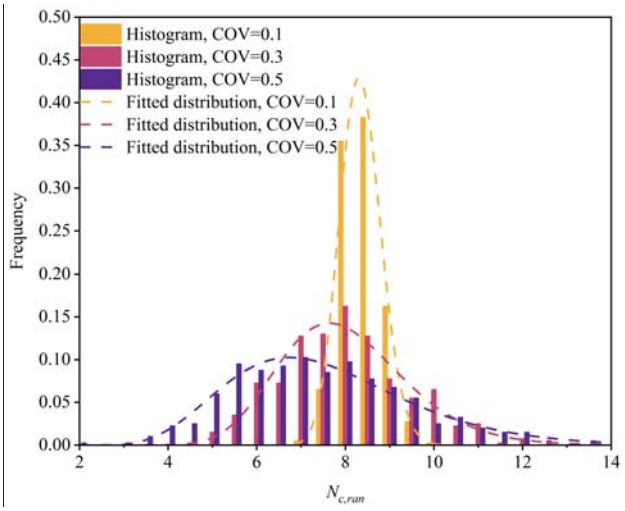

Figure 8. Histogram and fitted probability distribution of $N_{c,ran}$ for plate anchor with various COV (s_{ui}).

Since the $N_{c,ran}$ obeys the lognormal distribution, the 5th percentile value can be then estimated, as shown in Figure 9, with both the mean value and 5th percentile of $N_{c,ran}$ decrease with the increasing of COV (s_{ui}). Similar findings were also reported by Li et al. (2017).

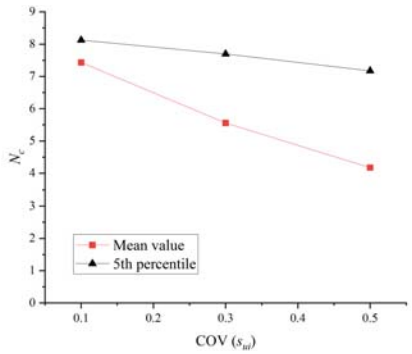

Figure 9. Variation in mean value and 5th percentile of capacity factor $N_{c,ran}$ for plate anchor with different of COV (s_{ui}).

4 Conclusion

This paper reported a three-dimensional random large deformation finite element study on the pull-out capacity of two typical anchors in spatially varied clay with different degrees of variation. The strain softening behavior of soil was taken into account by an extended Tresca constitutive model.

In both torpedo and plate anchor cases, the soli flow mechanism when failure occurs was found largely altered by the spatial variety of the soil, which further lead to the variation of the pull-out capacity. Increasing heterogeneity of soils results in more significant variation of the pull-out capacity and consequently a more serious reduction of 5th percentile of pull-out capacity.

References

Api, R. (2011) Design and analysis of stationkeeping systems for floating structures. Recommended practice API-RP-2SK. *American Petroleum Institute.*

Cassidy, M., Uzielli, M. and Tian, Y. (2013) Probabilistic combined loading failure envelopes of a strip footing on spatially variable soil. *Computers and Geotechnics* 49:191-205.

Chen, Z., Sun, J. and Gu, H. (2016) Inclined pull-out capacity of dynamically installed anchors in clay. *In Offshore Technology Conference Asia. OnePetro.*

Chen, Z., Tho, K. K., Leung, C. F. and Chow, Y. K. (2013) Influence of overburden pressure and soil rigidity on uplift behavior of square plate anchor in uniform clay. *Computers and Geotechnics* 52:71-81.

Chen, J., Leung, C. F., Chen, Z., Tho, K. K., & Chow, Y. K. (2015). Centrifuge model study on pullout behavior of plate anchors in clay with linearly increasing strength. *In Frontiers in Offshore Geotechnics III: Proceedings of the 3rd International Symposium on Frontiers in Offshore Geotechnics* (ISFOG 2015) (Vol. 1, pp. 839-844). Taylor & Francis Books Ltd.

De Sousa, J. R. M., De Aguiar, C. S., Ellwanger, G. B., Porto, E. C., Foppa, D. and De Medeiros, C. J. (2011) Undrained load capacity of torpedo anchors embedded in cohesive soils. *Journal of Offshore Mechanics and Arctic Engineering* 133(2).

Fu, Y., Yi, J. T., Li, Y. P. and Li, B. (2019) A semi-theoretical method for holding capacity of dynamically installed anchors under inclined loading. *Computers and Geotechnics* 115:103171.

Fu, Y., Zhang, X., Li, Y., Gu, H., Sun, J., Liu, Y. and Lee, F. H. (2017) Holding capacity of dynamically installed anchors in normally consolidated clay under inclined loading. *Canadian Geotechnical Journal* 54(9):1257-1271.

Griffiths, D. V., Fenton, G. A. and Manoharan, N. (2002) Bearing Capacity of Rough Rigid Strip Footing on Cohesive Soil: Probabilistic Study. *Journal of geotechnical and geoenvironmental engineering* 128(9):743-755.

Hossain, M., O'loughlin, C. and Kim, Y. (2015) Dynamic installation and monotonic pullout of a torpedo anchor in calcareous silt. *Géotechnique* 65(2):77-90.

Hossain, M. S., Kim, Y. and Gaudin, C. (2014) Experimental investigation of installation and pullout of dynamically penetrating anchors in clay and silt. *Journal of geotechnical and geoenvironmental engineering* 140(7):04014026.

Li, L., Li, J., Huang, J. and Gao, F. (2017) Bearing capacity of spudcan foundations in a spatially varying clayey seabed. *Ocean Engineering* 143:97-105.

Liu, Y., Lee, F. H., Quek, S. T. and Beer, M. (2014) Modified linear estimation method for generating multi-dimensional multi-variate Gaussian field in modelling material properties. *Probabilistic Engineering Mechanics* 38:42-53.

O'beirne, C., O'loughlin, C., Wang, D. and Gaudin, C. (2015) Capacity of dynamically installed anchors as assessed through field testing and three-dimensional large-deformation finite element analyses. *Canadian Geotechnical Journal* 52(5):548-562.

Phoon, K.-K. and Kulhawy, F. H. (1999) Characterization of geotechnical variability. *Canadian Geotechnical Journal* 36(4):612-624.

Tho, K. K., Chen, Z., Leung, C. F. and Chow, Y. K. (2014) Pullout behaviour of plate anchor in clay with linearly increasing strength. *Canadian Geotechnical Journal* 51(1):92-102.

Yi, J. T., Fu, Y., Liu, C. F., Zhang, Y. H., Li, Y. P. and Zhang, X. Y. (2020) Pull-out capacity of an inclined embedded torpedo anchor subjected to combined vertical and horizontal loading. *Computers and Geotechnics* 121:103478.

Zhu, D., Griffiths, D., Huang, J. and Fenton, G. (2017) Probabilistic stability analyses of undrained slopes with linearly increasing mean strength. *Géotechnique* 67(8):733-746.